PROCEEDINGS OF SCIENCE

Measurement of J/ψ, Υ and b-hadron production in proton-proton collisions at $\sqrt{s}$ = 7 TeV

R. Covarelli*
on behalf of the CMS collaboration
CERN, Switzerland
E-mail: roberto.covarelli@cern.ch

Measurements of the J/ψ and Υ production cross sections in proton-proton collisions at 7 TeV by the CMS experiment are presented. The dimuon decay channel is used for both analyses. For the J/ψ, inclusive differential cross sections versus transverse momentum are reported in two rapidity regions, as well as the b-hadron fraction, by separating the two contributions through a fit to the lifetime distribution, using the distance between the dimuon vertex and the interaction point. For the Υ, the (1S) cross section and the [(2S)+(3S)]/(1S) cross-section ratio are presented, both versus transverse momentum.

The Xth Nicola Cabibbo International Conference on Heavy Quarks and Leptons,
October 11-15, 2010
Frascati (Rome) Italy

*Speaker.

PoS(HQL 2010)011

1. Quarkonium physics at the CMS experiment

The CMS detector [1] at the LHC is a multi-purpose detector, primarily designed for the search of the Standard Model Higgs boson and New Physics in the high transverse momentum (p_T) region. Due to the versatility of the detector, especially of the High-Level Trigger system, and to the excellent muon resolution down to low-p_T values, interesting measurements in the field of quarkonium physics are also possible. Because of the typically large cross sections associated to these processes, and the relatively low instantaneous luminosity in the LHC start-up phase, a large sample of quarkonium decaying to dimuons has been effectively collected by the CMS muon triggers. The first results could therefore be obtained with the data recorded in 2010.

1.1 The High-Level Trigger

The CMS High-Level Trigger (HLT) [2] runs on an asynchronous farm of commercial CPUs on the events accepted by the Level-1 trigger decisions: it has access to event data with full granularity, allowing for precise object reconstruction and energy/momentum evaluation. At this step muon reconstruction and selection can be already performed with matching of different sub-detectors. At the lowest pp interaction rates, HLT for quarkonium physics is only based on single low-p_T muon objects and double muons at Level 1. Before moving to the double-muon High-Level Triggers, intermediate *ad-hoc* solutions are adopted, where full reconstruction of both muons is not required, but particular states (e.g. the J/ψ meson) can be selected with loose cuts on the invariant mass of a HLT muon and a Level-1 muon, or a HLT muon and a charged track.

1.2 Offline muon reconstruction

In CMS muon candidates are defined as tracks reconstructed in the silicon tracker and associated to a compatible signal in the muon chambers. Two different muon types are available in CMS [3].

The first one, referred to as a *Global Muon*, provides high-purity reconstruction for muons with $p_T \gtrsim 4$ GeV/c in the central pseudo-rapidity region, and $p_T \gtrsim 1$ GeV/c in the forward region. Global Muons are built as a combined fit of silicon and muon-chamber hits, belonging to independent tracks found in the tracker and muon systems.

The second muon type, referred to as a *Tracker Muon*, achieves a better reconstruction efficiency at lower momenta. The requirements for a Tracker Muon are looser than for Global Muons, at the expense of a slightly larger background: tracks found in the Tracker matched to only one muon segment are accepted and not refitted. If two (or more) tracks are close to each other, it is possible that the same muon segment or set of segments is associated to more than one track. In this case the best track is selected based on the angular matching between the extrapolated track and the segment in the muon detectors.

2. Quarkonium production cross section

From the theoretical point of view, the quarkonium cross section in hadron-hadron collision is still a debated topic. The discrepancy between TeVatron results [4] and the predictions of the Color Singlet Model (more reliable nowadays, due to recent theoretical developments [5]) has been solved

by introducing a Color Octet contribution, whose non-perturbative matrix elements have to be fitted from the experimental data [6]. Nevertheless, none of the two models has accounted simultaneously for the cross section and polarization measurements [7]. Charmonium is also interesting because, at relatively high p_T, a significant fraction of the J/ψ comes from b-hadron decays and, if it can be experimentally separated from the "prompt" component, provides a direct measurement of the $b \to J/\psi$ production cross section [8].

Inclusive charmonium and bottomonium events in CMS are reconstructed in the $Q\bar{Q} \to \mu^+\mu^-$ channel. Experimentally, the differential cross-sections can be expressed as:

$$\frac{d\sigma}{dp_T}(Q\bar{Q}) \cdot \mathrm{BR}(Q\bar{Q} \to \mu^+\mu^+) = \frac{N_{\mathrm{rec}}(Q\bar{Q})}{\int \mathscr{L} dt \cdot \langle A \cdot \varepsilon \rangle \Delta p_T} \tag{2.1}$$

where $N_{\mathrm{rec}}(Q\bar{Q})$ is the $Q\bar{Q}$ yield, in a given p_T bin, $\int \mathscr{L} dt$ is the integrated luminosity, $\langle A \cdot \varepsilon \rangle$ is the average value of the geometrical acceptance times the reconstruction efficiency of the di-muon in the p_T bin, and Δp_T is the size of the bin. In the J/ψ case, multiplication by $1 - f_B$ (f_B) in the bin gives the prompt (non-prompt) component of the total inclusive cross section.

Cross-section results are largely dependent on the quarkonium polarization, as different polarizations cause different muon momentum spectra in the laboratory frame. Given the sizeable extent of this effect, for prompt quarkonium (where the polarization is presently not well understood [9]) the final results are determined for different polarization scenarios, instead of treating this effect as a source of systematic uncertainty.

3. Determination of inclusive cross sections

The determination of *inclusive* cross sections for J/ψ [10] and Υ [11] mesons is performed based on a similar strategy, as detailed in the following paragraphs.

3.1 Data set and event selection

Samples of 100 ± 11 (280 ± 30) nb^{-1} proton-proton data, recorded at a center-of-mass energy of 7 TeV, are used for the J/ψ (Υ) cross-section analyses. Events are selected online by a double-muon trigger that requires the detection of two independent muon segments at Level 1, without any further processing at the HLT.

Signal Monte Carlo (MC) events of prompt J/ψ, non-prompt J/ψ and $\Upsilon \to \mu^+\mu^-$ are used to tune the selection criteria, to check the agreement with data, to compute the acceptance, to derive templates for the non-prompt J/ψ effective lifetime, and to derive corrections to the data-driven muon efficiencies. Detector conditions and trigger are included in the full simulation of these samples.

Muon tracks are required to pass the following requirements: they must have at least 12 hits in the tracker, at least two of which are required to be in the pixel layers, a track fit with a χ^2 per degree of freedom smaller than four, and must be closer to the primary vertex than 3 cm in the trasverse direction and 25 cm along the z-axis. In the Υ analysis, a minimum muon p_T is also required, depending on the muon pseudo-rapidity. A di-muon candidate is accepted if the di-muon vertex probability is larger than 0.001 and its invariant mass is in the J/ψ or the Υ mass regions.

3.2 Yield determination

Reconstructed yields are determined in bins of p_T using fits to the di-muon invariant mass distributions. In the case of Υ, a single rapidity region is considered ($|y| < 2.0$) while, in the case of J/ψ, statistics is sufficient to use two different rapidity regions: "central" ($|y| < 1.4$) and "forward" ($1.4 < |y| < 2.4$).

The mass peaks are described by Crystal Ball functions [12] in order to account for bremsstrahlung effects. In the Υ case, due to the presence of three partially overlapping states, some parameters (relative mass resolutions, global mass scale, α and n of the Crystal Ball functions) are constrained to be the same for the three peaks. Empirical (exponential or polynomial) functions are used to model the backgrounds.

Fig. 1 shows the result of the fits in the two mass regions, integrated over p_T for illustrative purposes.

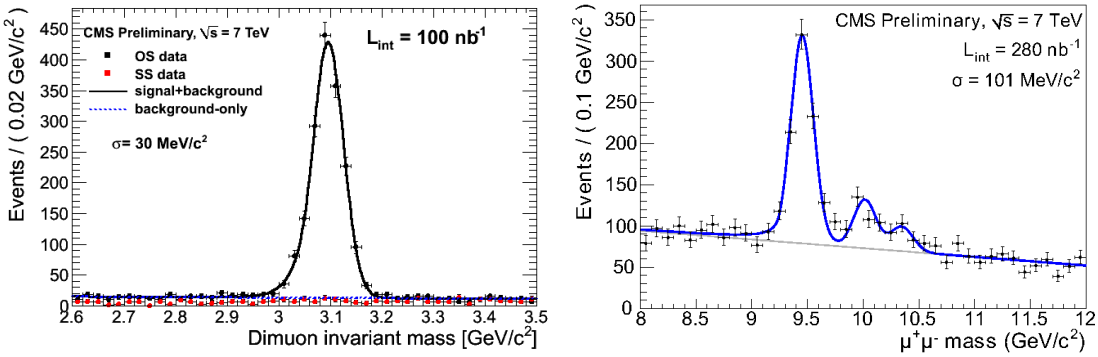

Figure 1: Di-muon invariant mass distributions with superimposed fits. Left: J/ψ mass region, $|y| < 1.4$; total and background-only fits are represented respectively by solid black and dashed blue lines. Right: $Y(nS)$ mass region, $|y| < 2.0$; total and background-only fits are represented respectively by solid blue and shaded grey lines.

3.3 Geometrical acceptance and muon efficiencies

Geometrical detector acceptance is determined from MC, generating events in the full kinematical phase space. Due to the large MC statistics available, statistical uncertainties on the acceptance are negligible. Several systematic effects have been evaluated, the dominant ones coming from the uncertainty in the amount of final-state radiation, on the muon momentum scale and on the measured uncertainty of the polarization of J/ψ from B decays. Uncertainty on the polarization of the prompt component is not treated as a systematic uncertainty, as explained in Sec. 2, but calculated for five benchmark scenarios.

Muon trigger and reconstruction efficiencies are determined from the data using the "tag-and-probe" method, which utilizes well-known dimuon decays to provide a sample of "probe" objects. A well-identified muon, called "tag", is combined with a second object in the event and the invariant mass is computed. The tag-probe pairs are divided into two samples, depending on whether the probe satisfies or not the criteria for the efficiency under consideration. The two tag-probe mass distributions contain a peak, the integral of which is the number of probes that satisfy or fail the

imposed criteria. The efficiency is extracted from a simultaneous unbinned maximum-likelihood fit to both mass distributions. In the Υ analysis, the available sample is not large enough to allow a precise determination of the efficiencies via the tag-and-probe method, and the J/ψ resonance is used.

The statistical uncertainties in the muon efficiencies determined with the tag-and-probe is used as a systematic uncertainty in the final results. The hypothesis that the di-muon efficiency factorizes into the product of single muon efficiencies is tested using MC and a corresponding systematic uncertainty is assigned.

3.4 Results

Inclusive differential cross-section results are derived for the J/ψ in 4 p_T bins in the central region and 9 in the forward region, here extending down to zero transverse momentum. Integrated in the region of full CMS acceptance ($4 < p_T < 30$ GeV/c, $|y| < 2.4$), the total cross section is obtained:

$$BR(J/\psi \to \mu^+\mu^-) \cdot \sigma(pp \to J/\psi + X) = 289 \pm 17(\text{stat}) \pm 60(\text{syst}) \text{ nb.}$$

Inclusive differential cross-section results for the Υ are only derived for the 1S state in 6 p_T bins. Fig. 2, top, shows these results compared to several theoretical and MC models: the CASCADE generator in the FONLL framework [13], PYTHIA, and the color evaporation model (CEM) [14]. The integrated result for $p_T < 20$ GeV/c, $|y| < 2.0$ is:

$$BR(\Upsilon(1S) \to \mu^+\mu^-) \cdot \sigma(pp \to \Upsilon(1S) + X) = 8.3 \pm 0.5(\text{stat}) \pm 1.3(\text{syst}) \text{ nb.}$$

The quantity R is also computed:

$$R = \frac{\sigma(pp \to \Upsilon(2S) + X) + \sigma(pp \to \Upsilon(3S) + X)}{\sigma(pp \to \Upsilon(1S) + X)} = 0.44 \pm 0.06(\text{stat}) \pm 0.07(\text{syst})$$

where the smaller systematic uncertainty reflects the cancellation of many systematic sources in the ratio.

4. Prompt and non-prompt J/ψ cross sections

4.1 Fraction of J/ψ from B decays

In the J/ψ analysis, separation of prompt and non-prompt events is achieved using the distribution of the "pseudo-proper decay length" $\ell_{J/\psi} = L_{xy} \cdot m_{J/\psi}/p_T$, where $m_{J/\psi}$ is the J/ψ mass and L_{xy} is the most probable transverse decay length in the laboratory frame, defined as $L_{xy} = (\mathbf{u}^T\sigma^{-1}\mathbf{x})/(\mathbf{u}^T\sigma^{-1}\mathbf{u})$. In the previous formula, $\mathbf{x}$ is the distance between the vertex of the two muons and the beam-crossing point of the event, computed on a run-by-run basis (in the transverse plane), $\mathbf{u}$ is the unit vector of the J/ψ p_T and σ is the sum of the beam-crossing point and di-muon vertex covariance matrices.

To determine the fraction f_B of J/ψ from b-hadron decays, a simultaneous unbinned maximum-likelihood fit to the dimuon mass spectrum and the $\ell_{J/\psi}$ distribution is performed in bins of p_T. For the mass distributions, the same functions of Sec. 3.2 are used. The decay length distributions are

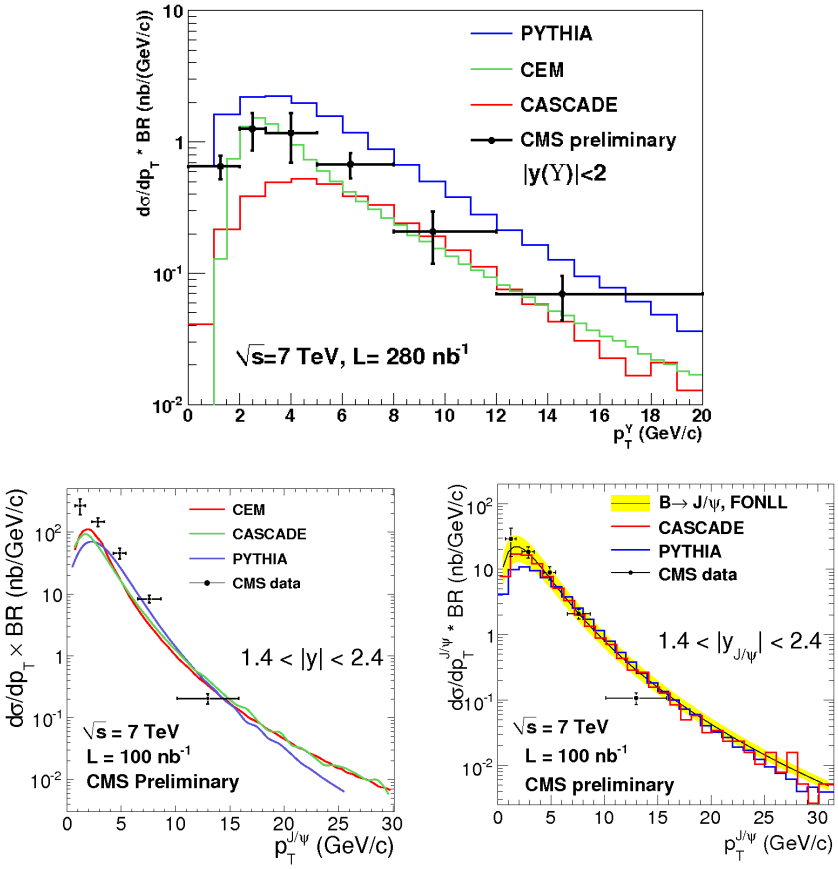

Figure 2: Measured differential cross-sections for $\Upsilon(1S)$ in the full rapidity region, (top) prompt J/ψ (bottom left), and non-prompt J/ψ (bottom right) in the forward region, compared to theoretical calculations (color lines).

described by: a simple 3-Gaussian resolution function for the prompt signal events; a MC template true distribution convolved with the resolution, for non-prompt signal events; a generic superposition of prompt and long-lived effective components for the background, whose parameters are determined from the mass sidebands. The result of one of these fits is shown in Fig. 3.

The statistical uncertainties obtained on f_B are of the order of 20%. The most important systematic sources are: tracker misalignment, the choice of the resolution model and the non-prompt decay length description, and the determination of the run-by-run primary vertex.

4.2 Results

Differential cross-section results are derived for the prompt and non-prompt J/ψ in 3 p_T bins in the central region and 5 in the forward region, using the b-fraction values, and are compared to theoretical predictions in Fig. 2, bottom, showing a good agreement except for the low p_T region. Integration over p_T and rapidity gives, for the non-prompt cross section:

$$BR(J/\psi \to \mu^+\mu^-) \cdot \sigma(pp \to b\bar{b} \to J/\psi + X) = 56.1 \pm 5.5(\text{stat}) \pm 7.2(\text{syst}) \text{ nb},$$

in $4 < p_T < 30$ GeV/c, $|y| < 2.4$.

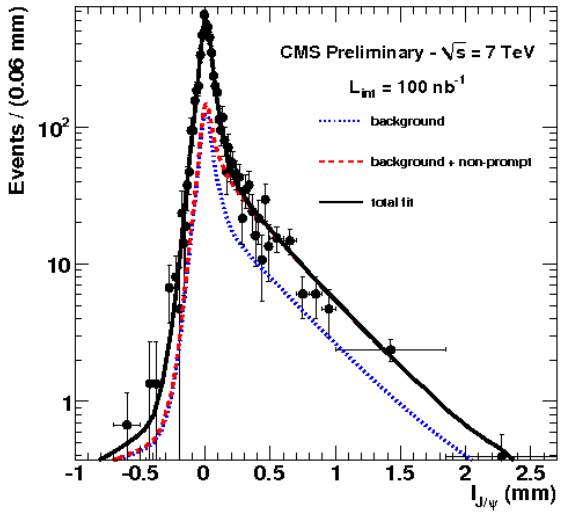

Figure 3: Measured $\ell_{J/\psi}$ distribution and likelihood fit result for the bin $6 < p_T < 10$ GeV/c, $|y| < 1.4$. The blue dotted line represents the background component only, the red dashed line includes the non-prompt component and the black line represents the total fit.

References

[1] The CMS Collaboration, S. Chatrchyan *et al.*, JINST **3**, S08004 (2008).

[2] The CMS Collaboration, "CMS High Level Trigger", CERN/LHCC 2007-021 (2007).

[3] The CMS Collaboration, "Performance of muon identification in pp collisions at $\sqrt{s}$ = 7 TeV", CMS-PAS MUO-10-002 (2010).

[4] The CDF Collaboration, D. Acosta *et al.*, Phys. Rev. **D71**, 032001 (2005).

[5] J.-P. Lansberg, Int. J. Mod. Phys. A **21**, 3857 (2006).

[6] G.T. Bodwin, E. Braaten and G.P. Lepage, Phys. Rev. **D51** 1125 (1995).

[7] The CDF Collaboration, T. Aaltonen *et al.*, Phys. Rev. Lett. 99, 132001 (2007).

[8] M. Cacciari, M. Greco and P. Nason, *JHEP* 9805, 007 (1998); M. Cacciari *et al.*, *JHEP* 0407, 033 (2004).

[9] P. Faccioli *et al.*, Eur. Phys. J. **C69**, 657 (2010).

[10] The CMS Collaboration, "J/ψ prompt and non-prompt cross sections in pp collisions at $\sqrt{s}$ = 7 TeV", CMS-PAS BPH-10-002 (2010).

[11] The CMS Collaboration, "Upsilon production cross sections in pp collisions at $\sqrt{s}$ = 7 TeV", CMS-PAS BPH-10-003 (2010).

[12] M.J. Oreglia, Ph.D. Thesis, SLAC-R-236, Appendix D (1980).

[13] H. Jung, Comp.Phys.Commun. 143, 100 (2002).

[14] F. Halzen, Phys. Lett. **B69**, 105 (1977); H. Fritzsch, Phys. Lett. **B67**, 217 (1977); M. Gluck, J.F. Owens and E. Reya, Phys. Rev. **D17**, 2324 (1978); V.D. Barger, W.-Y. Keung and R.J.N. Phillips, Phys. Lett. **B91**, 253 (1980).